POLARITON EFFECTS IN TRANSIENT GRATING EXPERIMENTS PERFORMED ON ANTHRACENE SINGLE CRYSTALS

Todd S. ROSE, Vincent J. NEWELL, Jeffrey S. METH and M.D. FAYER
Department of Chemistry, Stanford University, Stanford, CA 94305, USA

Received 19 January 1988

Excited state dynamics in anthracene crystals at low temperatures are studied with the transient grating technique. In contrast to work reported earlier, the excitation wavelength is in the vicinity of the polariton stop band, and there is a pronounced dependence of the time response on the wavelength. A qualitative discussion of the wavelength dependence of the grating transients is presented.

1. Introduction

The study of excited state dynamics and energy transport phenomena in molecular crystals has been an ongoing area of investigation for the past several decades. Single crystals of anthracene have received a great deal of experimental and theoretical attention. Despite the exhaustive research that has been conducted on this material, there are many fundamental questions that remain unanswered. To understand the dynamical properties of anthracene and other molecular solids, researchers have begun to employ time-resolved non-linear optical techniques. However, under certain circumstances, a clear interpretation of these types of experiments can be difficult due to the complex optical properties of the materials being investigated. In the low-temperature regime, where the coupling between the electromagnetic field and the media can be significant, excited state energy transport is a function of the combined electromagnetic and material field system.

At high temperatures, excited state energy transport in molecular crystals is incoherent. An optical excitation is essentially localized on a given site in the lattice and randomly hops from site to site. As the temperature of the material is decreased, phonon interactions are reduced and coherent states of the system become increasingly important. The eigenstates of the crystal are no longer localized site states, but are delocalized exciton states. In this situation, energy transport is discussed in terms of the propagation of exciton wave packets. Recent experiments on anthracene at very low temperatures (<10 K) have shown, however, that exciton theory alone is inadequate in describing the excited state dynamics [1–7]. Additional considerations concerning the strong coupling between the material and electromagnetic fields require the inclusion of Maxwell's equations into the problem. Energy transport needs to be described in terms of polaritons, which are the eigenstates of the crystal-field system.

Previously, Rose, Righini and Fayer [8] reported the first transient grating experiments performed on anthracene single crystals. In this work, the transient grating technique was employed to measure exciton transport at low temperatures. The studies measured the exciton diffusion constant at three different temperatures. The shapes of the grating decays and the temperature dependence of the diffusion constant indicated that the exciton coherence length was substantially larger than the lattice spacing, but smaller than the grating fringe spacing. The shape of the transient grating signal for different degrees of exciton coherence has been studied theoretically by Kenkre and Tsironis [9] and by Garrity and Skinner [10]. In an effort to produce excitons with very large coherence lengths, possibly on the order of the grating fringe spacing, experiments were performed in which the grating excitation pumped the S_1 level directly. (Previous experiments accessed S_1 via an ex-

0 009-2614/88/$ 03.50

cited vibrational level.) In this Letter, we report the results of these studies, which dramatically differ from those in ref. [8] because of polariton effects. Some of the considerations in the analysis of these kinds of experiments in terms of the polariton framework are discussed.

2. Experimental procedures

The details of the grating experiment can be found in ref. [8] and will only be described briefly in the text and in fig. 1. In contrast to the earlier experiments [8], the excitation and probe pulses were all the same wavelength (degenerate four wave mixing) and were tuned in the vicinity of the transverse polariton frequency ($\approx$398 nm). The wavelengths, recorded from a 3/4 meter monochromator, were not corrected for the vacuum. Calibration used the 313.1 nm mercury line. All of the wavelengths are relatively correct but could have a systematic error up to 2 cm^{-1}. The pulses were 30 ps in duration, had a bandwidth of 2 cm^{-1} and were derived by mixing the 1.06 μm of a Q-switched mode-locked Nd:YAG with the output of a synchronously pumped dye laser. The anthracene crystals were grown by subliming zone-refined anthracene at 130°C under 100 Torr of argon. The sublimation flakes ranged from 0.5 to a few μm thick and were mounted in a strain free holder. Fringe spacing dependences and wavelengths studies were performed at 1.8 K with the pulses polarized along the $\vec{b}$ crystallographic axis and the grating k vector oriented along the $\vec{b}$ crystallographic axis.

3. Results

The detailed shapes of the transient grating decay signals were found to be strongly dependent on experimental conditions, thus making any quantitative analysis in terms of the fringe spacing dependence uncertain. However, the general shapes of the grating decays were observed to be strongly correlated with the experimental wavelength. The wavelength dependence of the grating signal at a fringe spacing of 4.7 μm is shown in fig. 2. The data show delay times ranging between 0 and 1.5 ns. The wavelength

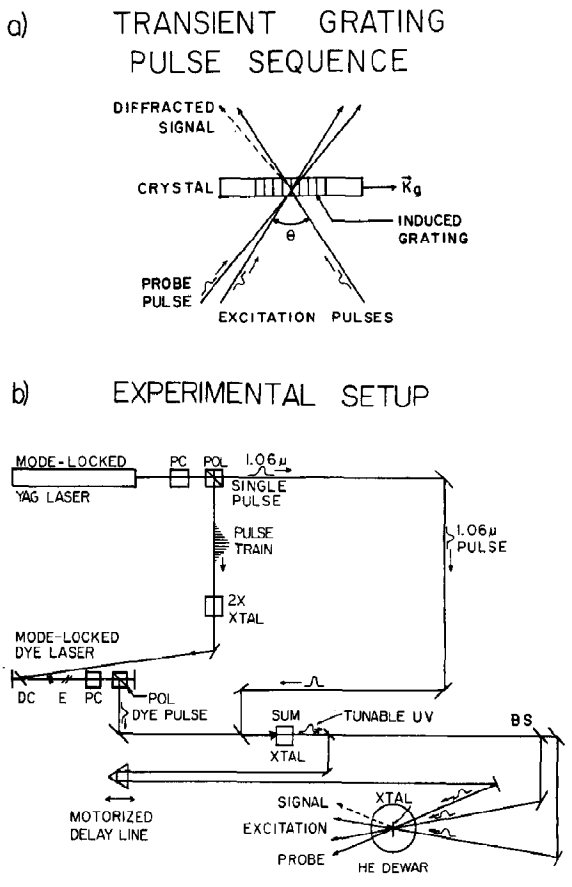

Fig. 1. (a) Schematic illustration of the transient grating experiment. Two coherently related excitation pulses cross in the sample and produce an optical interference pattern. Interaction of the radiation field with the sample results in a spatially sinusoidally varying concentration of excitations. This acts as a diffraction grating for the variably delayed probe pulse. K_g is the gravity wave vector. (b) The transient grating experimental arrangement. PC≡Pockels cell; POL≡polarizer; DC≡dye cell; E≡etalon; BS≡beamsplitter. A single Nd:YAG 1.06 μm picosecond pulse is selected from the pulse train with a Pockels cell. The leftover 1.06 μm pulse train is doubled, and the 532 nm pulse train synchronously pumps a dye laser. A cavity-dumped dye laser single pulse is summed with the 1.06 μm single pulse to produce tunable UV excitation and probe pulses. Time delay of the probe is achieved with a motorized delay line.

listed with each curve is the wavelength of the excitation and probe pulses. The progression shown in this figure was seen for most of the samples with a slight wavelength variation from crystal to crystal. No consistent dependence of the signal on the sample thickness was apparent. The main point to note from the results is that the grating decay shows two

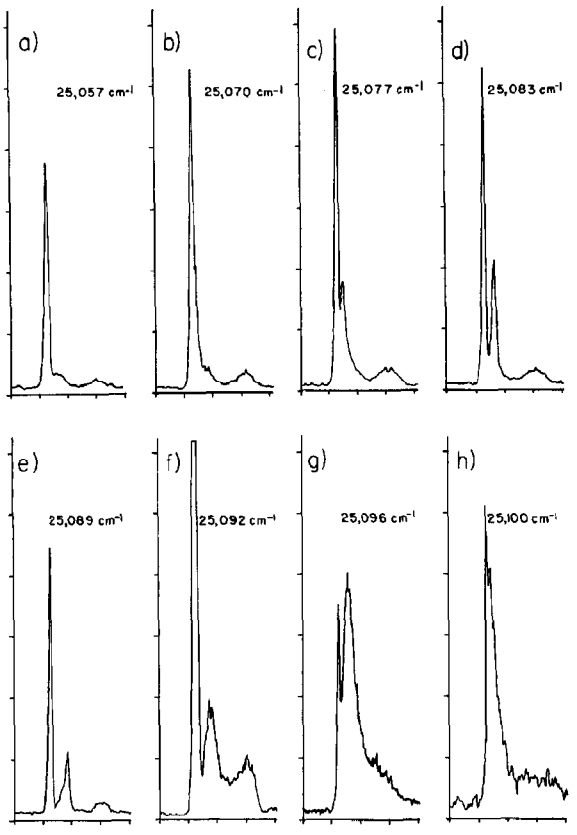

Fig. 2. Wavelength dependence of transient grating signal decays at a fringe spacing of 4.7 μm. The tick marks on the horizontal axis are every 0.5 ns. As the wavelength progresses to the blue, a new time delayed feature grows in.

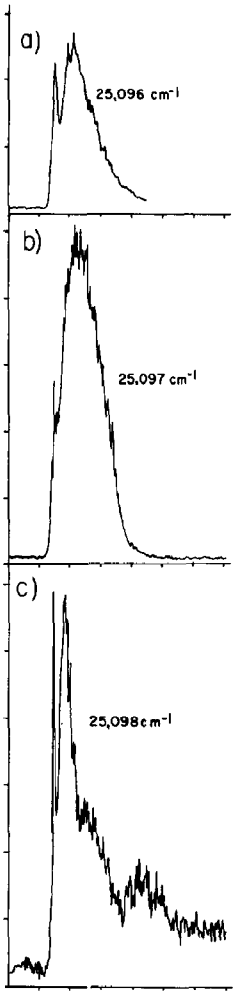

Fig. 3. Wavelength dependence of the signal decays at a fringe spacing of 3.4 μm. The tick marks on the horizontal axis are every 0.5 ns. (a) is at the same wavelength as fig. 2g. Although the fringe spacing is different, the decays are qualitatively similar. Wavelength changes of only 1 cm^{-1} result in dramatic changes in the time dependence of the grating signal.

distinct features: one which is sharp and one which is broad. The latter structure is extremely sensitive to the wavelength of the grating pulses and reaches its maximum intensity around 25097 cm^{-1}. To the red of the stop band, the broad component is reduced in size, as well as width, and essentially vanishes at wavelengths 30 cm^{-1} or more from the origin. It also exhibits oscillations which do not appear to arise from an acoustic phonon grating [8,11].

Fig. 3 shows a higher wavelength resolution in the vicinity of the region of greatest wavelength sensitivity. These data sets were at a fringe spacing of $d=3.4$ μm. The data in fig. 3a are at the identical wavelength as the data in fig. 2g. Notice that they are qualitatively the same. There is a sharp peak followed by a delayed broad peak of comparable intensity. Oscillations are not apparent. The broad feature in fig. 3a is significantly wider than in fig. 2b. Fig. 3b displays data taken one wavenumber to the blue. The broad feature is much larger and has a change in shape. Fig. 3c displays data taken an additional wavenumber to the blue. Here, the broad feature is considerably narrower and oscillations have become apparent. This demonstrates the tremendous sensitivity of the grating decays to the wavelength in this wavelength region.

The two components observed in the grating decays can result from two distinct polariton popula-

tions. The fast component is indicative of the decay of the initially generated polariton distribution, while the latter could be evidence of the buildup of polaritons in the "bottle-neck" region via acoustic phonon scattering. The existence of bottle-neck phenomena in anthracene is well documented both theoretically and in luminescence and Raman experiments [4,5,7]. In the grating experiment, the two excitation beams generate an initial ensemble of polaritons. Near the edge of the stop band, where the polariton dispersion is small, the polaritons possess low group velocities. These polaritons have a relatively high probability of scattering from optical or acoustic phonons before exiting the crystal. Scattering with optical phonons will tend to place the polariton on the light like portion of the dispersion curve. These polaritons possess relatively high group velocities and have a good chance of exiting the crystal before undergoing further scattering. On the other hand, polaritons which scatter off of acoustic phonons are still slow moving and have a high probability of undergoing further scattering. The successive scattering by acoustic phonons leads to imprisonment of the polaritons and the formation of population in the bottle-neck region. This secondary distribution may give rise to the broad structure observed in the grating transients. As the grating wavelength is tuned away from the stop band (see fig. 2), the strength of the grating diffraction arising from the secondary distribution is diminished because of the decrease in the acoustic phonon scattering frequency. Polaritons which are generated nearer to the light line of the dispersion curve are not readily scattered by phonons at low temperature because energy and momentum cannot be conserved.

A second similar, but distinct, explanation would still describe the initial fast feature as diffraction of the probe from what amounts to a polariton grating. As the frequency is tuned to the edge of the stop band the probability of polaritons damping into excitons increases. Unlike luminescence or Raman, the grating observable is sensitive to changes in the real and imaginary components of the index of refraction. Therefore, the grating experiment can be sensitive to states, such as excitons, which are not radiatively coupled to the ground state. In this picture, the slow component near 25097 cm^{-1} is an exciton grating which grows in as polaritons decay into excitons. Theoretical work [9,10] has suggested that the generation of coherent excitons near $k=0$ can lead to oscillations in the exciton grating decay. However, the theoretical work did not consider the consequences of the production of an exciton grating by polariton damping.

The influence of phonon scattering as a function of wavelength on polariton dynamics in anthracene has also been observed in the resonance scattering experiments of Aaviksoo et al. [7]. Time-resolved measurements on the emission from an 81 cm^{-1} Raman line at various excitation wavelengths were performed. The fast and slow components that were observed in their data were attributed to the two different polariton populations discussed above. The fast component resulted from polariton states which were populated via single scattering events of the initial polariton distribution with optical phonons. The slow component was derived from multiple scattering events between the initial polariton distribution and acoustic phonons. The relative contributions of the two components were found to be dependent upon the excitation wavelength. In contrast to their results, the temporal profiles of the grating transients were much more sensitive to the wavelength. The Raman decays were sensitive to wavelength changes of five to ten wavenumbers. We found that by changing the wavelength by only one or two wavenumbers (see fig. 3), the shapes of the grating transients were substantially altered. This extreme sensitivity is not to be expected in view of the anthracene polariton dispersion curve. Our results suggest that additional considerations, such as damping of polaritons into excitons, are necessary to interpret the grating results. The strong wavelength dependence very near 25097 cm^{-1} might involve surface excitons which give rise to very sharp structures in the reflectance spectra of anthracene in the vicinity of the stop band [12]. Bulk–surface coupling could play a role in the formation and evolution of the grating.

It is interesting to compare the transient grating results presented here to those discussed in ref. [8]. In these earlier experiments (which were performed at 1.8, 10, and 20 K), the two 355 nm excitation pulses, which formed the grating, created population in the second vibrational level of the 1430 cm^{-1} mode of S_1. The grating was probed by a third time-delayed pulse, whose wavelength range was 395 nm.

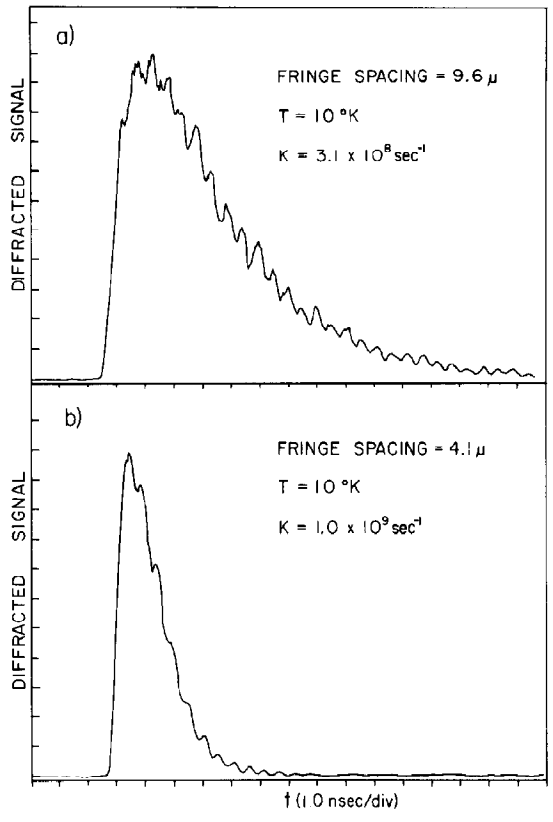

Fig. 4. Typical transient grating decays for an anthracene crystal initially excited into an S_1 vibrational level at 10 K [8]. The upper curve corresponds to a fringe spacing of 9.6 μm and shows a decay constant of $3.1\times10^8\ s^{-1}$. The lower curve was observed for a fringe spacing of 4.1 μm; the decay constant is $1.0\times10^9\ s^{-1}$. The difference in the decay with fringe spacing arises from exciton transport. As the fringe spacing becomes smaller, it takes less time for the excitons to migrate from grating peaks to grating nulls, resulting in faster decays. Note the differences in the shapes of these decays compared to those in figs. 2 and 3.

Typical results from these earlier experiments are shown in fig. 4 [8] [#1]. (The rapid oscillations on the data arise because of an acoustic effect and are distinct from the oscillations seen in fig. 2 [8].) The difference between decays observed in the earlier set of experiments and the transients presented in this paper is dramatic. In the earlier experiments, it is thought that the initial excitation into an excited vibrational level of S_1, followed by rapid relaxation to S_1, results in the formation of excitons, rather than polaritons. Consequently, the earlier grating experiments probe the dynamics of excitons. Data, such as that shown in fig. 4, were employed in the evaluation of the exciton diffusion constant [8] and the exciton coherence length [15]. (Recently, the influence of radiative decay on the grating time dependence has been discussed by Agranovich et al. [16].)

The current grating results show that a simple interpretation of the grating dynamics in terms of exciton diffusion is inappropriate when the excitation pulses are resonant with S_1 and the temperature is at 1.8 K. In this situation, the coupling between excitons and photons must be taken into account. Consequently, the propagation of the excitation and probe pulses through the medium and their interaction via $\chi^{(3)}$ should be considered within the polariton framework. Furthermore, any quantitative analysis would have to involve the optical anisotropy of the anthracene crystal. This consideration is especially important for the grating experiment, since it is desirable to vary the fringe spacing by changing the angle of intersection between the excitation pulses. Another qualitative indication of the importance of polariton effects and crystal anisotropy is the following observation. Because the crystals are very thin, plus and minus orders of diffraction can be readily observed. However, we observed, for example, that at a certain angle the +1 diffraction order would vanish while the −1 diffraction remained strong. If the experiment is viewed as the diffraction of a polariton probe from a grating, then for certain wavelengths and directions, propagation of the diffracted signal may not be allowed in view of the polariton dispersion. Consequently, the diffraction will vanish.

It is clear from these experiments that additional studies of the wavelength, temperature, intensity and fringe spacing dependences are necessary to obtain quantitative information on polariton and exciton dynamics. However, before such information can be interpreted in detail, a theoretical treatment of the transient grating experiment in terms of polariton theory is required.

[#1] In our previous Letter we reported the value of the exciton diffusion constant along the $\hat{a}$ axis. The correct direction is actually the $\hat{b}$ axis. Our incorrect assignment resulted from a discrepancy in the literature concerning the orientation of the anthracene isogyre (which is observed when viewing a crystal under a microscope) with respect to the $\hat{a}$ and $\hat{b}$ crystallographic axes (see refs. [13,14]). Nakada [14] gives the correct orientation, yet he references Lipsett [13].

Acknowledgement

This work was supported by the National Science Foundation, Division of Materials Research (No. DMR84-16343).

References

[1] M.R. Philpott, J. Chem. Phys. 60 (1974) 2520; Chem. Phys. Letters 30 (1975) 387.
[2] J. Ferguson, Chem. Phys. Letters 36 (1975) 316; Z. Physik. Chem. B 101 (1976) 46.
[3] M.S. Brodin, M.A. Dudinskii, S.B. Marisova and E.N. Myasnikov, Phys. Stat. Sol. 74b (1976) 453.
[4] M.D. Galanin and Sh.D. Khan-Magometova, J. Luminescence 18/19 (1979) 37; Mol. Cryst. Liquid Cryst. 57 (1980) 119.
[5] N.A. Vidmont, A.A. Maksimov and I.I. Tartakovskiĭ, JETP Letters 37 (1983) 689; Soviet Phys. Solid State 24 (1982) 784.
[6] J. Aaviksoo, J. Lippmaa, A. Freiberg and A. Anijalg, Solid State Commun. 49 (1983) 115.
[7] J. Aaviksoo, A. Freiberg, T. Reinot and S. Savikhin, J. Luminescence 35 (1986) 267.
[8] T.S. Rose, R. Righini and M.D. Fayer, Chem. Phys. Letters 106 (1984) 13.
[9] V.M. Kenkre and G.P. Tsironis, J. Luminescence 82 (1985) 260.
[10] D.K. Garrity and J.L. Skinner, J. Chem. Phys. 82 (1985) 260.
[11] K.A. Nelson, R. Casalegno, R.J.D. Miller and M.D. Fayer, J. Chem. Phys. 77 (1982) 1144.
[12] J.M. Turlet, P.H. Kottis and M.R. Philpott, Advan. Chem. Phys. 54 (1983) 303.
[13] F.R. Lipsett, Can. J. Phys. 35 (1957) 284.
[14] I. Nakada, J. Phys. Soc. Japan 17 (1962) 113.
[15] V.M. Kenkre and D. Schmid, Phys. Rev. B 31 (1985) 2430.
[16] V.M. Agranovich, A.M. Ratner and M. Salieva, Solid State Commun. 63 (1986) 329.